E-layer is produced by pre-ionization and the fine structure of the *E*-layer, as reported recently,[12] is produced by intensifications of ionization due to high energy photons.

The author wishes to express his gratitude to Professor S. K. Mitra, for suggesting the problem and for constant help in the preparation of the paper. This paper forms a part of the work done in the scheme on "Ionospheric Investigations" financed by the Council of Scientific and Industrial Research, Government of India, and the author expresses his thanks to the Council for providing the necessary facilities for research work.

[12] R. Naismith, Wireless Eng. **28**, 271 (1951).

PHYSICAL REVIEW VOLUME 88, NUMBER 2 OCTOBER 15, 1952

The Backscattering of Positrons and Electrons

H. H. SELIGER
National Bureau of Standards, Washington, D. C.
(Received March 31, 1952)

Beta-rays from a point source, backscattered by materials of various atomic numbers Z have been collected over a 2π solid angle and also over narrow solid angles at various obliquities. In all cases electrons are backscattered to a greater extent than positrons. The number and energy spectrum of the backscattered beta-rays depend strongly on the direction of emergence and on Z. In spite of the use of hetero-energetic sources, the results can be interpreted qualitatively on the basis of multiple scattering, in terms of a "side-scattered" and a "diffused" component.

I. INTRODUCTION

THERE has been relatively little recent experimental work on the backscattering of fast electrons in matter and none on the backscattering of positrons. Brand[1] has studies the backscattering of cathode rays up to 32 kev in energy and Bothe[2] has extended the measurements to 680 kev using radioactive sources in a magnetic analyzer.

Recently the author reported an excess of electron backscattering over positron backscattering.[3] This excess of electron backscattering over positron backscattering is to be expected indirectly on the basis of the single scattering cross sections as calculated by Bartlett and Watson[4] for electrons and Massey[5] for positrons. A further study of the backscattering process has provided several very interesting results from which one is able to deduce a qualitative understanding of the general backscattering process.

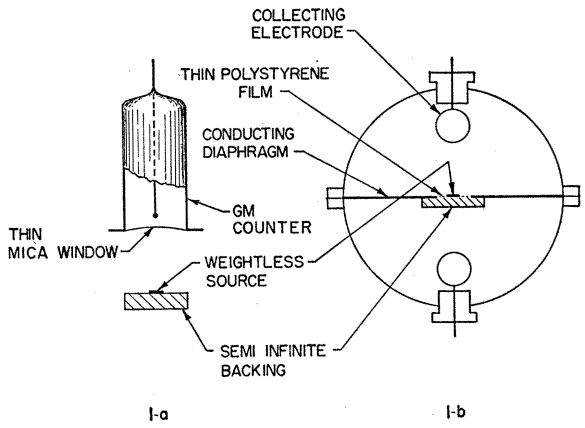

FIG. 1 (a). Schematic drawing of geometrical arrangement of the previously reported experiments; (b) schematic drawing of 4π counter arrangement.

[1] J. O. Brand, Ann. Physik **5**, 609 (1936).
[2] W. Bothe, Z. Naturforsch. **4a**, 542 (1949).
[3] H. H. Seliger, Phys. Rev. **78**, 491 (1950).

II. EXPERIMENTAL PROCEDURE

The geometry of the previous experiment (see reference 3) is indicated schematically in Fig. 1(a). If one defines an angle θ as the angle between the plane containing the front surface of the backing and the plane containing the axis of the detector and the source, then in Fig. 1(a), $\theta=90°$.

The present experiments can be divided into two parts. In the first part the backscattering coefficients for both positrons and electrons as functions of the atomic number Z of the backing material were measured for a 2π solid angle, in contrast with the solid angle of roughly 1 steradian in Fig. 1(a). These 2π backscattering coefficients were determined in 4π absolute beta-counters.[6] The geometry of the measurement is indicated schematically in Fig. 1(b). In the second part the angular distributions of the backscattered electrons and positrons, both in number and in energy, were measured as functions of Z. The arrangement of Fig. 1(a) was modified so that the solid angle subtended was only 0.01 steradian. The source approximated a point source, and the backing on which the source was

[4] J. H. Bartlett and R. E. Watson, Proc. Am. Acad. Arts Sci. **74**, 53 (1940).
[5] H. S. W. Massey, Proc. Roy. Soc. (London) **A181**, 14 (1942).
[6] H. H. Seliger and L. Cavallo, Natl. Bur. Standards J. Research **47**, 41 (1951).

mounted was constructed so that it could rotate, with its axis of rotation laying in the plane of the front surface of the backing and perpendicular to the line containing the axis of the detector. Thus by rotation of the backing relative to the counter one could sample the backscattered radiation at various angles θ. Estimates of the energy distribution of the backscattered electrons were made by means of absorption curves in aluminum. These absorption curves, extrapolated to zero total absorber, also gave the correction for the absorption due to the thickness of air and counter window.

P^{32}(E_{max} 1.71 Mev) and Na^{22}(E_{max} 0.58 Mev) were used as sources of negative and positive electrons, respectively. The backscattering was measured for Lucite, aluminum, copper, silver, platinum, and lead.

1. 2π Backscattering Coefficients

The 2π backscattering coefficients were measured in the following manner: The absolute disintegration rate of the source, N_0 was determined in the 4π counter by the method outlined in reference 6. Then the source, mounted on a thin polystyrene film, was placed on the polished face of the backing and the counting rate in the top half of the counter was measured. This is given by

$$N_t'=\tfrac{1}{2}N_0[1+\beta(1-\tau)^2], \qquad (1)$$

where N_t' is the counting rate in the top half of the 4π counter, β is the backscattering coefficient, and τ is the fractional absorption in the mounting film ($\tau \ll 1$). The factor $(1-\tau)$ is taken squared because a particle must pass through the mouting film twice if it is backscattered. The procedure for determining τ is also given in reference 6. β, defined by (1) can be written as

$$\beta=\frac{1}{(1-\tau)^2}\left[\frac{N_t'-\tfrac{1}{2}N_0}{\tfrac{1}{2}N_0}\right]. \qquad (2)$$

$\tau \sim 0$ for P^{32} electrons, so that β reduces to

$$\beta=(2N_t'/N_0)-1. \qquad (3)$$

In the case of Na^{22} positrons τ is not zero and a further correction is necessary because of the associated γ and annihilation radiation. It is possible that a γ or annihilation quantum accompanying a positron which is stopped in the backing will produce a count in the top half of the 4π counter, thereby making β^+ appear larger than the true value. The presence of cascade or annihilation radiation does not affect the determination of N_0 since the entire process occurs well within the resolving time of the proportional counter and amplifier for the original beta-particle ionization pulse.

A new set of 4π counter equations was derived, following the same line of reasoning as in the original paper on 4π counting, but this time taking into account the γ and annihilation radiation from the Na^{22} positrons. The final result for β gave

$$\beta=\frac{1}{(1-\tau)^2}\left[\frac{N_t'-\tfrac{1}{2}(N_0+N_b')}{\tfrac{1}{2}(N_0-N_b')}\right], \qquad (4)$$

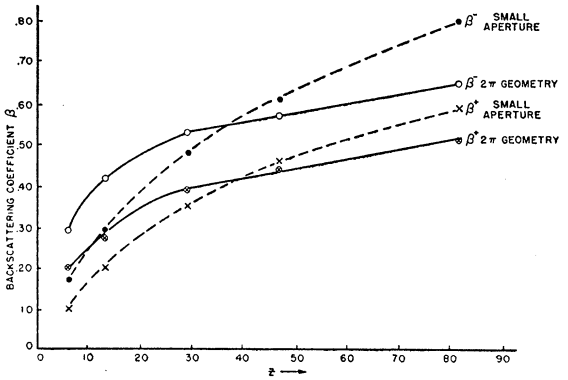

FIG. 2. Backscattering coefficients for positrons and electrons as functions of Z, measured with 2π geometry (solid curves) compared with previously measured backscattering coefficients.

where N_b', the counting rate in the bottom half of the 4π counter with the infinite backing in place, is due entirely to the effect of the photons. The total correction, including that for film absorption and for γ and annihilation radiation, amounted to roughly 5 percent.

Another possible correction involved in the case of the Na^{22} positrons is introduced by the finite probability that a positron will be annihilated in motion. However, even in the case of lead, this probability is of the order of 1 or 2 percent.[7] For lower Z it would be still smaller. No corrections were made for this effect.

2. Angular Distribution Measurements

An arrangement was used here whereby the point source was evaporated on a thin film and supported below the detector. The backing could be brought up directly in contact with the thin film and then backing and film could be rotated so as to sample the radiation at various angles θ. A complete absorption curve in aluminum was measured for the source mounted on the thin film with no backing behind it. The angular distribution of this unscattered or direct radiation was effectively isotropic from $\theta=+10°$ to $\theta=-10°$, the limiting angular range of the experimental arrangement. A slight asymmetry due to difficulty in exact centering of the source was present, but the average of the values for plus and minus θ removed this effect. Next, similar absorption curves were measured for $\theta=\pm 10°$, $\pm 20°$, $\pm 30°$, $\pm 60°$, and 90° with the various backings in position. At each angle θ, the difference between the latter set of readings and the former or unscattered readings gave the net backscattered radiation reaching the detector through that particular absorber. These differences plotted as functions of the thickness of aluminum absorber represent the absorption of the net backscattered radiation. Corrections were made in the case of Na^{22} for the γ-ray background.

[7] W. Heitler, *Quantum Theory of Radiation* (Oxford University Press, London, 1947), second edition, p. 231.

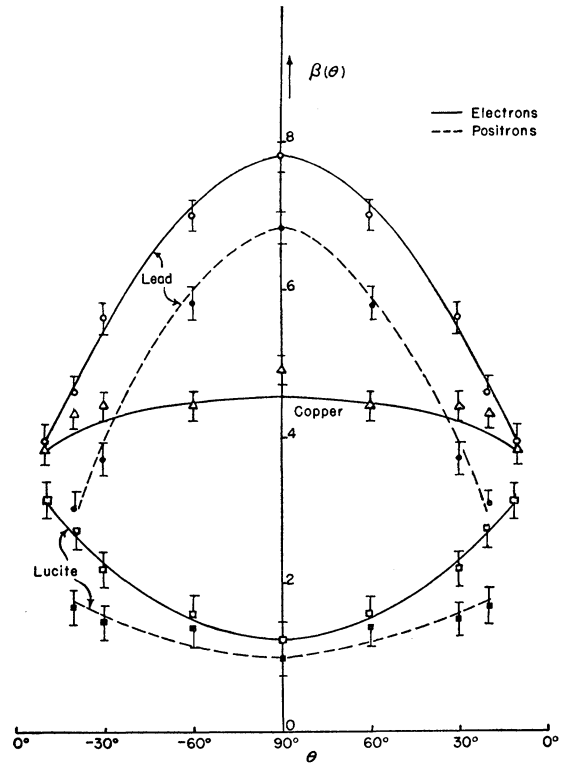

FIG. 3. Angular distribution of the backscattering coefficients for positrons and electrons for high, medium, and low Z backing materials.

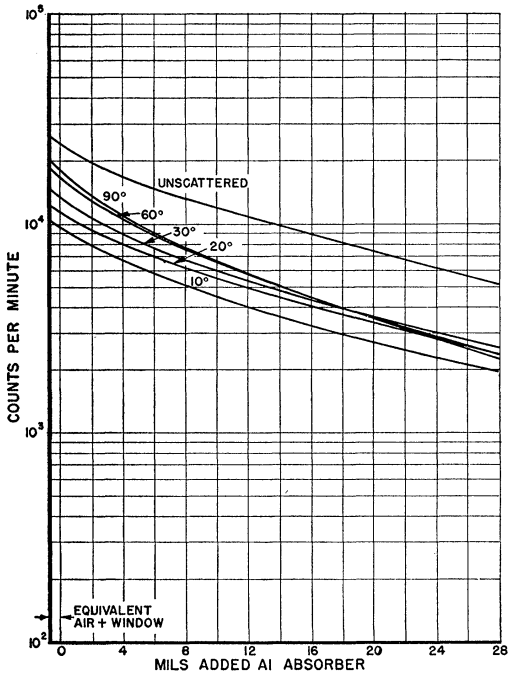

FIG. 4. Absorption in aluminum of the net backscattered P^{32} electrons from a lead backing. The unscattered absorption curve is shown for comparison.

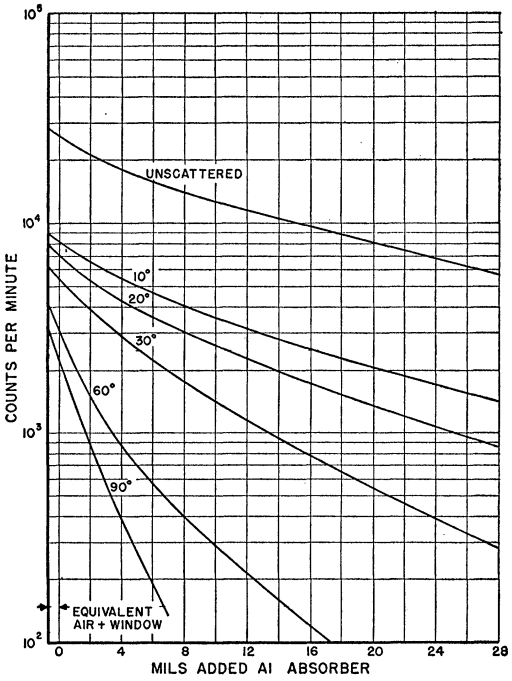

FIG. 5. Absorption in aluminum of the net backscattering P^{32} electrons from a Lucite backing. The energy loss can be estimated by comparison with the unscattered absorption curve.

III. RESULTS

Except for quantitative values, the positrons exhibited the same characteristics as electrons so that the discussion will be limited to electrons.

The final results for the 2π backscattering coefficients as measured in the 4π counter are shown by the solid lines in Fig. 2. The dashed line curves are the results of the previous measurement with the geometry of Fig. 1(a). The differences in backscattering between the two

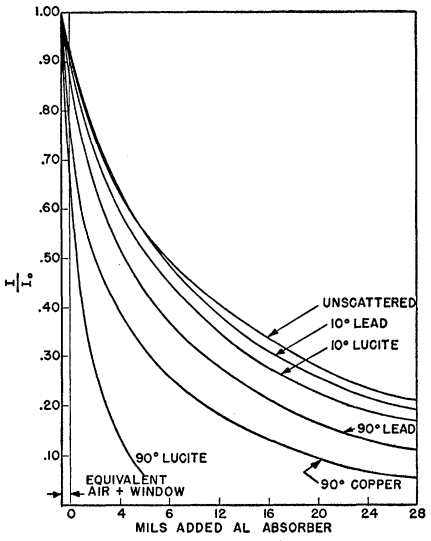

FIG. 6. Relative transmission of P^{32} backscattered electrons from low, medium, and high Z for $\theta=10°$ and $\theta=90°$.

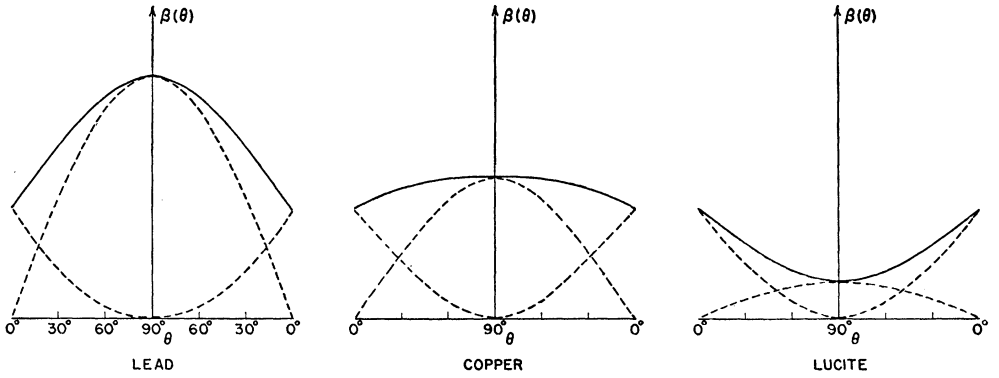

FIG. 7. Relative contributions to $\beta(\theta)$ of the diffusion effect (concave downward dashed curves) and the side scattering effect (concave upwards dashed curves), assuming a cosine distribution for the diffusion effect. The solid lines are taken from Fig. 3 for electrons.

types of geometries and especially the lower values of β at high Z and higher values of β at low Z measured over the 2π solid angle point up the anisotropy of the angular distribution of the backscattered radiation. The magnitude of this anisotropy is shown more clearly in Fig. 3, where the backscattering coefficient β is plotted as a function of the angle θ. Here $\beta(\theta)$ is defined by

$$\beta(\theta)=N(\theta)/N_u, \tag{5}$$

where $N(\theta)$ is the net extrapolated backscattered radiation at the angle θ, and N_u is the extrapolated value of the unscattered radiation, both at zero total absorber. From the $\beta(\theta)$ curves of Fig. 3 one can infer the results of Fig. 2, since

$$\langle\beta(\theta)\rangle_{Av}=\int_0^{\pi/2}\beta(\theta)\cos\theta d\theta.$$

Therefore, $\langle\beta(\theta)\rangle_{Av}<\beta(90°)$ for high Z and $\langle\beta(\theta)\rangle_{Av}>\beta(90°)$ for low Z. In addition to the values of $N(\theta)$, the absorption curves in aluminum of the net backscattered radiation give very important results concerning the relative energy degradation of the backscattered particles as functions of θ and of Z. Figures 4 and 5 show curves representing the absorption of P^{32} electrons backscattered from lead and from Lucite, respectively.

It is seen that electrons emerging at $\theta=90°$ from low Z materials are tremendously degraded in energy while those emerging at $\theta=10°$ are only slightly degraded. In the case of high Z materials the electrons emerging at $\theta=90°$ are only slightly different in energy from those emerging at 10°. The relative energy degradation as a function of θ and Z is brought out more clearly by Fig. 6 where the fractional transmission from lead, copper, and Lucite backings is plotted for $\theta=10°$ and $\theta=90°$. Here one can see that the particles emerging at small angles θ have a similar energy spectrum to the original unscattered electrons, while the spectrum of those emerging at large angles θ is quite different and has a large Z dependence.

IV. DISCUSSION

An important feature and a fortunate simplification in the interpretation of the present experimental results is the fact that the backscattering is approximately energy independent in the energy range considered. This was shown in abundant detail by Brand[1] and Bothe[2] for monoenergetic electrons and by Burtt,[8] Zumwalt,[9] and the author[3] for hetero-energetic radioactive sources with widely differing end points. Blanchard and Fano have shown[10] that the shape of the distribution function which describes the angular distribution of an electron inside a scatterer with respect to its original direction at any point along its path depends on the energy loss E_0-E and the original energy E_0 principally as the ratio $(E_0-E)/E_0$. Although a 100-kev electron beam will penetrate deeper into a scatterer than a 50-kev electron beam, both beams will lose their original "sense" of direction, or become isotropic at the same fractional loss of energy. Therefore the same fraction of each should be reflected in any given Z element. However, the ratio of elastic to inelastic scattering is proportional to Z, so that an electron in a high Z material will become isotropic with much less energy loss than it would in a low Z material, thereby increasing its probability of escape from the high Z material. The angular distribution of diffusing electrons emerging from any plane surface follows a cosine φ law where the angle φ is defined by $\varphi=(90°-\theta)$.

A qualitative estimate of the diffusion effect can be obtained by normalization of the experimental curves of Fig. 3 to a cosine distribution at $\theta=90°$. In Fig. 7 this is represented by the dashed concave downward curves. The difference between the experimental or solid line curves in Fig. 7 and the cosine distribution curves is given by the dashed concave upward curves. This distribution is due to the incompletely diffused or sidescattered electrons. Electrons initially incident and subsequently emerging at small angles with the surface lose only a small fraction of their original energy in being deflected and it is to those electrons that the adjective "side scattered" is applied. Since the ratio of scattering to absorption cross sections is still proportional to Z, the sidescattered electrons will lose less energy in the high Z material than in the low Z material. However, since little energy is lost even in low Z materials, the degradation for the sidescattering effect will be very much less than the degradation for the complete diffusion effect. In Fig. 6 the 10° transmission

[8] B. P. Burtt, Nucleonics 5, No. 2, 28 (1949).
[9] L. R. Zumwalt, unpublished report Mon C 397 (1950).
[10] C. H. Blanchard and U. Fano, Phys. Rev. 82, 767 (1951).

curves show that electrons sidescattered from Lucite are only slightly less energetic than those sidescattered from lead, while at 90° electrons diffusing from Lucite are almost totally degraded, being very much lower in energy than electrons diffusing from lead.

Figure 7 indicates that the diffusion effect increases materially with Z while the side scattering remains relatively constant. It can be argued that at small angles of incidence and emergence, while the mean deflection necessary for emergence will be reached after many more collisions in a low Z material than in a high Z material, the electron has roughly the same probability of emerging from a low Z material as from a high Z material, although it will be slightly less energetic upon emerging from the low Z material.

Miller[11] has made calculations of the ratio β^-/β^+, using Bartlett and Watson's and Massey's cross section calculations in a classical multiple scattering theory originally given by Bothe[12] for electrons. He estimates $\beta^-/\beta^+=1.16$ for mercury. The experimental results show $\beta^-/\beta^+=1.3$ for $Z=80$, which is in fair agreement with Miller's results, especially since the initial conditions in Bothe's derivation are not exactly those of the present experiments. In any case an excess of electron backscattering over positron backscattering is to be expected.

The isotropic initial conditions of the experiments are those most commonly encountered in actual practice in radioactivity measurements. It is therefore quite important to recognize that the backscattering is anisotropic, so that the proper backscattering correction can be made, depending on the geometry used. The curves of Fig. 2 should be especially helpful to those working with C^{14}, S^{35} and other low energy beta-emitters, where a 2π windowless counter is often used.

The author wishes to thank Miss L. Cavallo and Miss S. V. Culpepper for their valuable assistance in making these measurements, and Dr. U. Fano and Dr. C. H. Blanchard for many stimulating and enlightening discussions.

[11] W. Miller, Phys. Rev. **82**, 452 (1951).
[12] W. Bothe, Ann. Physik **6**, 44 (1949).

PHYSICAL REVIEW VOLUME 88, NUMBER 2 OCTOBER 15, 1952

Thermal Neutron Capture Cross Sections

H. POMERANCE
Oak Ridge National Laboratory, Oak Ridge, Tennessee
(Received June 11, 1952)

The thermal neutron capture cross sections of more than one hundred isotopes, including all the isotopes of 24 elements, plus several others, have been measured with the Oak Ridge National Laboratory pile oscillator.

THE thermal neutron capture cross sections of the elements have been measured by many techniques, but the cross sections for the individual isotopes[1] of those elements have been determined for the most part only by activation methods. Activation methods may be used only with roughly half of all stable isotopes, namely, those that become radioactive upon thermal neutron capture, and other techniques must be used for the remainder. A few measurements have been made by determining with a mass spectrometer the depletion produced by prolonged neutron bombardment, and some measurements have recently been made by counting directly the neutron capture gamma-rays; in both these methods natural samples can be employed. This paper reports on work with the Oak Ridge National Laboratory pile oscillator, which can measure directly the thermal neutron capture of any stable isotope sample. The more than one hundred enriched isotopic samples used in these measurements were produced by electromagnetic separation in the Stable Isotope Research Division of Oak Ridge National Laboratory.

[1] Cross section values with bibliographical references may be found in *Nuclear Data*, Nat. Bur. Standards Circular No. 499 (1950).

The pile oscillator has been previously described and has been used to measure the cross sections of 69 elements.[2] It operates by pulsing the current of a boron-coated ionization chamber by moving the sample back and forth through the chamber, and by integrating these pulses which are proportional to the capture area of the sample. By operating in the reflector of the graphite reactor, the pile oscillator uses principally thermal neutrons; the cadmium ratio on indium is about 30, indicating that even for as unfavorable a case as indium the nonthermal capture contributions are at most 3.2 percent. The thermal capture cross sections for the isotopes as for the elements have been measured relative to gold for which the cross section has been taken to have a value of 95 barns for neutrons of 2200 m/sec velocity.[2]

The values of the isotopic cross sections are listed in Table I. The isotopic cross sections are for the pure isotopes; the atomic cross sections listed in the last column are the contributions of the isotopes to the natural elements and are found by multiplying the isotopic cross sections by the natural relative abundances. The errors are estimated from the average per-

[2] H. Pomerance, Phys. Rev. **83**, 641 (1951).